Experimental and Theoretical *ab Initio* Study of the $^{13}C-^{13}C$ Spin−Spin Coupling and ^{1}H and ^{13}C Shielding Tensors in Ethane, Ethene, and Ethyne

Jaakko Kaski, Perttu Lantto, Juha Vaara, and Jukka Jokisaari*

Contribution from the NMR Research Group, Department of Physical Sciences, University of Oulu, FIN-90571 Oulu, Finland

Received August 20, 1997. Revised Manuscript Received December 8, 1997

Abstract: Experimentally and theoretically (*ab initio*) determined CC spin−spin coupling tensors and ^{1}H and ^{13}C nuclear shielding tensors are reported for ethane ($^{13}C_2H_6$), ethene ($^{13}C_2H_4$), and ethyne ($^{13}C_2H_2$). The experimental anisotropies of the CC coupling tensors, ΔJ_{CC}, for all these molecules, and also the combination $J_{CC,xx} - J_{CC,yy}$ for ethene, were derived from sets of anisotropic couplings (D^{exp}) analyzed from the ^{1}H and ^{13}C NMR spectra of molecules partially oriented in liquid−crystalline environments. Both harmonic vibrations and structural deformations arising from the correlation of vibrational and reorientational motions were taken into account in the *D* couplings. The *ab initio* calculations of all the **J** tensors were performed using MCSCF linear response theory. The best calculated and experimental ΔJ_{CC} values (along with $J_{CC,xx} - J_{CC,yy}$ for ethene) are found to be in good mutual agreement. Together with earlier work on the $^{n}\mathbf{J}_{CC}$ tensors in benzene, this study shows that the indirect contribution, $^{1}/_{2}J_{CC}^{aniso}$, to experimental couplings between differently hybridized carbons is small and can generally be omitted. This means that the use of experimental D_{CC} couplings in the determination of molecular order tensors and/or conformation does not introduce serious errors. The experimental determination of the ^{1}H and ^{13}C shielding tensors was based on the liquid crystal director rotation by 90° in mixtures of thermotropic nematogens with opposite anisotropy of diamagnetic susceptibility. *Ab initio* SCF and MCSCF calculations utilizing gauge-including atomic orbitals produce results in good agreement with experiments.

Introduction

The nuclear shielding tensor, $\boldsymbol{\sigma}$, and the indirect spin−spin coupling tensor, **J**, are responses of the molecular electronic system to the magnetic fields of NMR spectrometer (an external source) and magnetic nuclei, respectively. When measured in isotropic solutions, molecular tumbling averages the tensors to scalar numbers $\sigma = \sigma^{iso}$ and $J = J^{iso}$, the shielding and spin−spin coupling constants, respectively. Thus, information on the individual tensor elements $T_{\alpha\beta}$ ($\mathbf{T} = \boldsymbol{\sigma}$ or **J**) is not available through NMR experiments performed in isotropic environments. On the contrary, when molecules are introduced in an anisotropic environment, the determination of the anisotropy of the tensor, $\Delta T = T_{zz} - {}^{1}/_{2}(T_{xx} + T_{yy})$, the difference $T_{xx} - T_{yy}$, and certain combinations of off-diagonal elements become feasible, depending on the symmetry of the solute.

NMR spectroscopy of molecules partially oriented in liquid−crystalline (LC) solutions (LC NMR) appears to be the most applicable experimental means to derive information on the **J** and $\boldsymbol{\sigma}$ tensors.[1,2] Unlike solid-state NMR[3] where small effects are masked by broad lines, the LC NMR method allows even the determination of small anisotropies reliably, provided that the effects of molecular vibrations[4] and medium-induced deformations[5] on the experimental anisotropic couplings, D^{exp}, as well as the solvent effects on nuclear shielding and spin−spin coupling, are properly taken into account.

Data on nuclear shielding tensor obtained using solid-state techniques with powder samples[6] correspond to the principal axis system (PAS) of the tensors, while the LC NMR observables refer to the PAS of the molecular orientation tensor. Transformation between these different presentations requires knowledge of the directions of the PAS axes of the shielding tensor, which is unavailable with powder NMR methods. Single crystal or dipolar techniques are needed to overcome this. Once the directions are known, the tensor is transformable to the molecule-fixed frame, and the comparison of the two sets of data becomes possible. The inverse transformation is not generally possible due to the lack of LC NMR information on the nondiagonal elements of the tensor in the molecule-fixed frame.

Independent, reliable determination of the $\mathbf{J}$[7−11] and σ[12−20] tensors by *ab initio* electronic structure calculations has become

* Author for correspondence: Department of Physical Sciences, University of Oulu, P.O. Box 333, FIN-90571 Oulu, Finland, Fax:+358-8-553 1287, Email:Jukka.Jokisaari@oulu.fi.

(1) Lounila J.; Jokisaari, J. *Prog. NMR Spectrosc.* **1982**, *15*, 249−90.
(2) Jokisaari, J. *Encyclopedia of NMR Spectroscopy*; John Wiley & Sons: New York, 1996; Vol. 2, pp 839−48.
(3) Wasylishen, R. E. *Encyclopedia of NMR Spectroscopy*; John Wiley & Sons: New York, 1996; Vol. 3, pp 1685−95.
(4) Sýkora, S.; Vogt, J.; Bösiger, H.; Diehl, P. *J. Magn. Reson.* **1979**, *36*, 53−60.
(5) (a) Lounila, J.; Diehl, P. *J. Magn. Reson.* **1984**, *56*, 254−61. (b) Lounila, J.; Diehl, P. *Mol. Phys.* **1984**, *52*, 827−45. (c) Lounila, J. *Mol. Phys.* **1986**, *58*, 897−918.
(6) Orendt, A. M. *Encyclopedia of NMR Spectroscopy*; John Wiley & Sons: New York, 1996; Vol. 2, pp 1282−97.
(7) Sekino, H.; Bartlett, R. J. *J. Chem. Phys.* **1986**, *85*, 3945−9. Salter, E. A.; Sekino, H.; Bartlett, R. J. *J. Chem. Phys.* **1987**, *87*, 502−9.
(8) (a) Galasso, V. *J. Chem. Phys.* **1985**, *82*, 899−904. (b) Galasso, V.; Fronzoni, G. *J. Chem. Phys.* **1986**, *84*, 3215−23.

S0002-7863(97)02936-3 CCC: $15.00
Published on Web 04/14/1998

feasible in recent years. Although often computationally demanding, these methods allow, at best, a quantitative comparison with experimental data for the coupling and shielding constants and also the tensorial properties. The latter are, however, seldom reported. Use of distributed gauge origins[12−15,21] and treatment of electron correlation[16−20] have become the standard in the modern theoretical approaches to the shielding tensor. First principles calculation of the **J** tensor facilitates breaking it into contributions arising from the different physical mechanisms: the dia- and paramagnetic spin−orbit (DSO and PSO), spin-dipole (SD), Fermi contact (FC), and the SD/FC cross-term contributions.[1] While the FC term often dominates J^{iso}, it contributes nothing to the anisotropic parts of **J**, contrary to the fully anisotropic SD/FC term.

We have previously investigated the ${}^{n}\mathbf{J}_{CC}$ ($n = 1, 2, 3$) tensors in benzene by the LC NMR method and *ab initio* multiconfiguration self-consistent field (MCSCF) linear response calculations.[22] The conclusion of the study was that the tensorial properties of these couplings give negligibly small contributions in view of the use of D_{CC}^{exp} in determinations of the orientation tensors[23] or geometries of molecules[24] containing phenyl groups in LC solutions. A corresponding comprehensive study is lacking for the series of simple hydrocarbons: ethane (C_2H_6), ethene (C_2H_4), and ethyne (C_2H_2), in which the carbon atoms are sp^3, sp^2, and sp hybridized, respectively. From the theoretical viewpoint these small molecules are more appealing objects of study than benzene, and a greater degree of agreement of *ab initio* results with experimental data is expected for them.

We are not aware of any LC NMR studies of ethane. On the contrary, both ethene and ethyne have been subjects of interest. The studies of ethene deal with the structure and the effect of the vibration−rotation interaction on the structure.[25,26] Also a rough estimate for the CC coupling anisotropy, 90 Hz, was reported.[25] The main emphasis in ethyne focused on the odd solvent and temperature effects on the structure and order tensor.[27,28] The extreme solvent and temperature sensitivity of the structure was in ref 27 explained on the basis of specific interactions between ethyne and LC molecules (Merck Phase 4). The situation was modeled using a two-site theory which allows ethyne to occupy two different environments in which it possesses slightly deviating structures and orientations.[27] Later, van der Est et al.[28] suggested that specific interactions and the two-site model are not needed provided that the vibration−rotation interaction is taken into account. Some small discrepancies in the *D* couplings were interpreted as arising from the anisotropy of the CC spin−spin coupling. The resulting ΔJ_{CC} values are, however, scattered over a wide range and, furthermore, disagree with both the experimental and theoretical results of the present study. Retreatment of the data of ref 28 performed presently brings the CC coupling anisotropies to the same level as obtained from our new experiments, however. The current experiments on ethyne in the Phase 4 LC show that the rotation−vibration interaction alone is not sufficient to explain the odd behavior of ethyne but clearly also specific interactions contribute. Therefore, we omit the data obtained in this particular LC.

Ethane, ethene, and ethyne were previously used as test molecules to investigate the dependence of the indirect HH, CH, and CC couplings on hybridization.[29] The ^{1}H and ^{13}C shielding anisotropies of ethyne, $\Delta\sigma_H$ and $\Delta\sigma_C$, were derived as early as in 1972 by applying LC NMR.[30,31] The corresponding data for ethene is given in ref 32. For the $\boldsymbol{\sigma}_C$ tensors of ethane, ethene and ethyne determined using solid-state NMR, see for example refs 33, 34, and 35, respectively.

First principles calculations of the *J* constants have been reported for these molecules a number of times.[8,11,36,37] Results for ΔJ in C_2H_2 and C_2H_4 have been published by Galasso and Fronzoni who used the equation-of-motion (EOM) method and 6-31G basis set.[8b] Semiempirical results are available for all the anisotropies.[38−40] It appears worthwhile to reinvestigate particularly the full $\mathbf{J}_{CC}$ tensors for these molecules by using modern *ab initio* methods and good basis sets. Theoretical ^{1}H and ^{13}C shielding tensors have recently been reported.[41−43] Accurate σ constants by the CCSD method were calculated by Gauss and Stanton.[44]

In the present study we report experimental LC NMR and theoretical ab initio results for the CC spin−spin coupling tensors and the ^{1}H and ^{13}C shielding tensors for $^{13}C_2H_6$, $^{13}C_2H_4$, and $^{13}C_2H_2$, including single, double, and triple CC bonds, respectively. In the analysis of the experimental *D* couplings,

(9) (a) Geertsen, J.; Oddershede, J. *Chem. Phys.* **1987**, *104*, 67−72. (b) Geertsen J.; Oddershede, J.; Scuseria, G. E. *J. Chem. Phys.* **1987**, *87*, 2138−42.
(10) Vahtras, O.; Ågren, H.; Jørgensen, P.; Jensen, H. J. Aa.; Padkjær, S. B.; Helgaker, T. *J. Chem. Phys.* **1992**, *96*, 6120−5.
(11) (a) Malkin, V. G.; Malkina, O. L.; Salahub, D. R. *Chem. Phys. Lett.* **1994**, *221*, 91−9. (b) Dickson, R. M.; Ziegler, T. *J. Phys. Chem.* **1996**, *100*, 5286−90.
(12) Kutzelnigg, W. *Isr. J. Chem.* **1980**, *19*, 193−200.
(13) Schindler, M.; Kutzelnigg, W. *J. Chem. Phys.* **1982**, *76*, 1919−33.
(14) Hansen, Aa. E.; Bouman, T. D. *J. Chem. Phys.* **1985**, *82*, 5035−47.
(15) Wolinski, K.; Hinton, J. F.; Pulay, P. *J. Am. Chem. Soc.* **1990**, *112*, 8251−60.
(16) Gauss, J. *J. Chem. Phys.* **1993**, *99*, 3629−43.
(17) Ruud, K.; Helgaker, T.; Kobayashi, R.; Jørgensen, P.; Bak, K. L.; Jensen, H. J. Aa. *J. Chem. Phys.* **1994**, *100*, 8178−85.
(18) Schreckenbach, G.; Ziegler, T. *J. Phys. Chem.* **1995**, *99*, 606−11.
(19) Malkin, V. G.; Malkina, O. L.; Erikson, L. A.; Salahub, D. R. In *Modern Density-Functional Theory: A Tool for Chemistry*, Vol. 2 of *Theoretical and Computational Chemistry*; Politzer, P., Seminario, J. M., Eds.; Elsevier: Amsterdam, 1995; p 273.
(20) Gauss, J.; Stanton, J. F. *J. Chem. Phys.* **1996**, *104*, 2574−83.
(21) Helgaker, T.; Jørgensen, P. *J. Chem. Phys.* **1991**, *95*, 2595−601.
(22) Kaski, J.; Vaara, J.; Jokisaari, J. *J. Am. Chem. Soc.* **1996**, *118*, 8879−86.
(23) Sandström, D.; Summanen, K. T.; Levitt, M. H. *J. Am. Chem. Soc.* **1994**, *116*, 9357−8.
(24) Sandström, D.; Levitt, M. H. *J. Am. Chem. Soc.* **1996**, *118*, 6966-8.
(25) Diehl, P.; Sýkora, S.; Wullschleger, E. *Mol. Phys.* **1975**, *29*, 305−6.
(26) Wasser, R.; Diehl, P. *Magn. Reson. Chem.* **1987**, *25*, 766−70.
(27) Diehl, P.; Sýkora, S.; Niederberger, W.; Burnell, E. E. *J. Magn. Reson.* **1974**, *14*, 260−9.
(28) van der Est, A. J.; Burnell, E. E.; Barnhorn, J. B. S.; de Lange, C. A.; Snijders, J. G. *J. Chem. Phys.* **1988**, *89*, 4657−65.
(29) Lynden-Bell, R. M.; Sheppard, N. *Proc. R. Soc. A* **1962**, *269*, 385−403.
(30) Englert, G. *Z. Naturforsch.* **1972**, *27a*, 1536−7.
(31) Mohanty, S. *Chem. Phys. Lett.* **1973**, *18*, 581−3.
(32) Diehl, P.; Moia, F. *Isr. J. Chem.* **1983**, *23*, 265−7.
(33) Solum, M. S.; Facelli, J. C.; Michl, J.; Grant, D. M. *J. Am. Chem. Soc.* **1986**, *108*, 6464−70.
(34) Zilm, K. W.; Conlin, R. T.; Grant, D. M.; Michl, J. *J. Am. Chem. Soc.* **1980**, *102*, 6672−6.
(35) Zilm, K. W.; Beeler, D. M.; Grant, D. M.; Michl, J.; Chou, T.-C.; Allred, E. L. *J. Am. Chem. Soc.* **1981**, *103*, 2119−20.
(36) Geertsen, J.; Oddershede, J. *Chem. Phys.* **1986**, *104*, 67−72.
(37) Perera, S. A.; Nooijen, M.; Bartlett, R. J. *J. Chem. Phys.* **1996**, *104*, 3290−305.
(38) Buckingham, A. D.; Love, I. *J. Magn. Reson.* **1970**, *2*, 338−51.
(39) (a) Nakatsuji, H.; Kato, H.; Morishima, I.; Yonezawa, T. *Chem. Phys. Lett.* **1970**, *4*, 607−10. (b) Nakatsuji, H.; Morishima, I.; Kato, H.; Yonezawa, T. *Bull. Chem. Soc. Jpn.* **1971**, *44*, 2010−7. (c) Facelli, J. C.; Barfield, M. *J. Magn. Reson.* **1984**, *59*, 452−68.
(40) Pyykkö, P.; Wiesenfeld L. *Mol. Phys.* **1981**, *43*, 557−80.
(41) Rizzo, A.; Helgaker, T.; Ruud, K.; Barszczewicz, A.; Jaszuński, M.; Jørgensen, P. *J. Chem. Phys.* **1995**, *102*, 8953−66.
(42) Chesnut, D. B.; *Chem. Phys.* **1997**, *214*, 73-9.
(43) Grayson, M.; Raynes, W. T. *Mol. Phys.* **1994**, *81*, 533−45.
(44) Gauss, J.; Stanton, J. F. *J. Chem. Phys.* **1995**, *103*, 3561−77.

contributions due to harmonic vibrations and structural deformations were taken into account. The nuclear shielding tensors for ethane and ethyne were determined using ENEMIX method[45] which is assumed to eliminate at least partially the effects due to solvent molecules on the nuclear shielding tensor. The *ab initio* calculations were performed using the MCSCF linear response theory[10] for the **J** tensors and the gauge-including atomic orbital (GIAO)[15,21,46,47] SCF and MCSCF theories[17] for the $\boldsymbol{\sigma}$ tensors. The present $^2\mathbf{J}_{CC}$ results, combined with our earlier work on the aromatic system,[22] complete the investigation of the CC coupling tensors in small model systems containing differently hybridized carbons.

LC NMR Observables

The NMR spin Hamiltonian appropriate for spin-$^1/_2$ nuclei in molecules partially oriented in uniaxial LC solvents can be written, in the high field approximation and in frequency units, as[2]

$$\hat{H} = -B_0/(2\pi)\sum_i \gamma_i(1-\sigma_i)\hat{I}_{iz} + \sum_{i<j} J_{ij}[\hat{I}_{iz}\hat{I}_{jz} + {}^1/_2(\hat{I}_{i+}\hat{I}_{j-} + \hat{I}_{i-}\hat{I}_{j+})] + \sum_{i<j}(2D_{ij} + J_{ij}^{\text{aniso}})[\hat{I}_{iz}\hat{I}_{jz} - {}^1/_4(\hat{I}_{i+}\hat{I}_{j-} + \hat{I}_{i-}\hat{I}_{j+})] \quad (1)$$

where B_0 is the external magnetic field flux density of the spectrometer (along the z axis of the laboratory frame), and γ_i, $\hat{\mathbf{I}}_i$, and σ_i are the gyromagnetic ratio, dimensionless spin operator, and nuclear shielding of a nucleus i, respectively. σ_i is a sum of isotropic and anisotropic contributions, $\sigma_i = \sigma_i^{\text{iso}} + \sigma_i^{\text{aniso}}$. We adopt a notation in which J_{ij} is used for J_{ij}^{iso} and σ_i for σ_i^{iso}; J_{ij}^{aniso} and σ_i^{aniso} are used explicitly when the anisotropic parts of the tensors are meant. The sign convention for the primary spectral observable, the chemical shift, is chosen as $\delta_i = \sigma_{\text{ref}} - \sigma_i$. The direct dipolar coupling D_{ij} is

$$D_{ij} = -\mu_0\hbar\gamma_i\gamma_j\langle s_{ij}/r_{ij}^3\rangle/(8\pi^2) \quad (2)$$

where rovibrational averaging is indicated by the angular brackets, $\langle s_{ij}\rangle = {}^1/_2\langle 3\cos^2\theta_{ij,\mathbf{B}_0} - 1\rangle = S_{ij}$ is the order parameter of the internuclear vector $\mathbf{r}_{ij}$ with respect to $\mathbf{B}_0$ (the angle between $\mathbf{B}_0$ and $\mathbf{r}_{ij}$ is $\theta_{ij,\mathbf{B}_0}$), and μ_0 and $\hbar$ have their usual meanings. The experimentally available couplings in a molecule dissolved into a LC, D_{ij}^{exp}, can be expressed as a sum of several contributions

$$D_{ij}^{\text{exp}} = D_{ij} + {}^1/_2 J_{ij}^{\text{aniso}} = D_{ij}^{\text{eq}} + D_{ij}^{\text{ah}} + D_{ij}^{\text{h}} + D_{ij}^{\text{d}} + {}^1/_2 J_{ij}^{\text{aniso}} \quad (3)$$

where D_{ij}^{eq} is the coupling corresponding to the equilibrium structure of the molecule, D_{ij}^{ah} arises from the anharmonicity of the vibrational potential,[48] D_{ij}^{h} is the contribution from the harmonic vibrations,[4] and D_{ij}^{d}, the deformational contribution, is due to the correlation between vibrational and reorientational motions.[5] The last contribution is responsible for the apparent solvent dependence of molecular geometry. In general, the isotropic and anisotropic parts of second rank NMR observables (either from **J** or $\boldsymbol{\sigma}$) can be presented as

$$T^{\text{iso}} = (T_{xx} + T_{yy} + T_{zz})/3 = (1/3)\text{Tr}\,\mathbf{T} \quad (4)$$

where Tr stands for trace, and

$$T^{\text{aniso}} = (2/3)P_2(\cos\theta)\sum_{\alpha\beta} S_{\alpha\beta}{}^D T_{\alpha\beta} \quad (5)$$

where $S_{\alpha\beta}{}^D = {}^1/_2\langle 3\cos\theta_{\alpha,\mathbf{n}}\cos\theta_{\beta,\mathbf{n}} - 1\rangle$ are the elements of the Saupe ordering tensor (in some molecule-fixed frame (α, β, γ)). P_2 is the second-order Legendre polynomial, and θ the angle between the external magnetic field and the LC director, **n**.

Experimental Section

NMR Spectroscopy. The compounds studied, i.e., ethane, ethene, and ethyne (all doubly ^{13}C labeled and delivered by ISOTEC Inc.), together with $^{13}CH_4$ serving as an internal chemical shift reference, were dissolved in several thermotropic LC solvents (all from Merck AG) which were placed in 8-mm o.d. NMR tubes (Wilmad) and predegassed in a vacuum line. The gases were introduced into the samples with the aid of liquid nitrogen, and the tubes were sealed with flame. The compositions of the LC solvents used are given in Table 1.

Ethane (pressure ca. 2.8 atm) was dissolved with methane (1.4 atm) in the LCs I−V, ethene (2.2 atm) with methane (1.8 atm) in the LCs I−VI, and ethyne (2.2 atm) with methane (1.8 atm) in the LCs I−IV. The anisotropy of the diamagnetic susceptibility, $\Delta\chi_m$, is negative in the LCs I, II, and VI, and therefore their director orients perpendicularly to the external magnetic field. In the other cases $\Delta\chi_m$ is positive, resulting in parallel orientation of **n** with $\mathbf{B}_0$. In particular, the mixture III has the property that the geometrical distortions of the solute molecules arising from the orienting anisotropic forces from the mesophase appear to be vanishingly small.[45]

The ^{1}H and ^{13}C NMR spectra of each sample were recorded on a Bruker Avance DSX 300WB spectrometer with a BB 10-mm probehead. D_2O, placed in the annulus of the concentric 10 and 8 mm tubes, was used as a locking substance. The spectra were recorded in isotropic and anisotropic phases at temperatures of 360 and 305 K, respectively. The typical run parameters were the following: 64 scans and 1.4 s acquisition time for ^{1}H and 1024 scans and 1.4 s for the ^{13}C spectrum in the common "π/6 flip angle − FID" method. The J constants were determined from spectra taken in the isotropic phase of each sample using the PERCH program.[49] They were kept fixed to these values during the PERCH analyses of the spectra taken in the anisotropic phases. The analyses resulted in very accurate values for the J and D couplings when applying the so-called "peak-top-fit" mode, absolute errors being a few hundreds of a hertz at maximum.

The anisotropies of the CC spin−spin coupling tensors, $\Delta J_{CC} = J_{CC,zz} - {}^1/_2(J_{CC,xx} + J_{CC,yy})$, for all the molecules, and the combination $J_{CC,xx} - J_{CC,yy}$ for ethene, were derived from the experimental D_{ij} couplings corrected for both harmonic vibrations and deformations applying the MASTER[50] program (as will be discussed below, the latter correction was not needed in the analysis of the ethyne data[51]). In the MASTER analysis at least one bond length (usually r_{CC}) must be fixed in order to scale the molecular size. The harmonic force fields of ethane, ethene and ethyne were adopted from refs 52, 53, and 54, respectively. For ethane it was essential to take into account the internal rotation of the methyl group around the CC bond. We have placed the z axis along the CC bond in all the molecules. The molecular plane of ethene is the xz plane.

***Ab Initio* Calculations.** The spin−spin coupling and shielding tensors were calculated using the DALTON software.[55] The theory

(45) Jokisaari, J.; Hiltunen, Y. *Mol. Phys.* **1983**, *50*, 1013−23.
(46) London, F. *J. Phys. Radium* **1937**, *8*, 397-409.
(47) Ditchfield, R. *J. Chem. Phys.* **1972**, *56*, 5688−91.
(48) Lounila, J.; Wasser, R.; Diehl, P. *Mol. Phys.* **1987**, *62*, 19−31.
(49) Laatikainen, R.; Niemitz, M.; Weber, U.; Sundelin, J.; Hassinen, T.; Vepsäläinen, J. *J. Magn. Reson.* A **1996**, *120*, 1−10.
(50) Wasser, R.; Kellerhals, M.; Diehl, P. *Magn. Reson. Chem.* **1989**, *27*, 335−9.
(51) Wasser, R.; Diehl, P. *J. Magn. Reson.* **1989**, *81*, 121−8.
(52) Duncan, J. L.; Kelly, R. A. *J. Mol. Spectrosc.* **1983**, *98*, 87−110.
(53) Martin, J.; Taylor, P. R. *Chem. Phys. Lett.* **1996**, *248*, 336−44.
(54) Strey, G.; Mills, I. M. *J. Mol. Spectrosc.* **1976**, *59*, 103−15.
(55) Helgaker, T.; Jensen, H. J. Aa.; Jørgensen, P.; Olsen, J.; Ruud, K.; Ågren, H.; Andersen, T.; Bak, K. L.; Bakken, V.; Christiansen, O.; Dahle, P.; Dalskov, E. K.; Enevoldsen, T.; Fernandez, B.; Heiberg, H.; Hettema, H.; Jonsson, D.; Kirpekar, S.; Kobayashi, R.; Koch, H.; Mikkelsen, K. V.; Norman, P.; Packer, M. J.; Saue, T.; Taylor, P. R.; Vahtras, O. *Dalton release 1.0, an electronic structure program*, 1997.

Table 1. Compositions of the Liquid Crystals Used[a]

no.	code name	composition
I	ZLI 1167	a mixture of three *p*(*n*-alkyl)*trans*,*trans*-bicyclohexyl-*p′*-carbonitriles; alkyl = propyl (36%), pentyl (34%), and heptyl (30%)
II	ZLI 1167 (80)/phase 4 (20)[b]	mixture consisting of 80 wt % ZLI 1167 and 20 wt % phase 4
III	ZLI 1167 (58)/phase 4 (42)	mixture consisting of 58 wt % ZLI 1167 and 42 wt % phase 4
IV	ZLI 1167 (30)/phase 4 (70)	mixture consisting of 30 wt % ZLI 1167 and 70 wt % phase 4
V	ZLI 1982	mixture of alkyphenylcyclohexanes, alkylcyclohexanebiphenyls, and bicyclohexanebiphenyls
VI	ZLI 2806	mixture of alkylbicyclohexanes and alkyltricyclohexanes

[a] All from Merck AG. [b] Phase 4: Eutectic mixture of *p*-methoxy-*p′*-(*n*-butyl)azoxydibenzenes.

Table 2. Atomic Orbital Basis Sets Used in the *Ab Initio* Calculations[a]

basis		Gaussian functions: GTO	Gaussian functions: CGTO	contraction pattern[b]
HIII	H	(6s2p)	[4s2p]	{3 3 × 1/2 × 1*}
	C	(11s7p2d)	[7s6p2d]	{5 6 × 1/2 5 × 1/2 × 1*}
HIV	H	(6s3p1d)	[5s3p1d]	{2 4 × 1/3 × 1*/1*}
	C	(11s7p3d1f)	[8s7p3d1f]	{4 7 × 1/7 × 1/3 × 1*/1*}

[a] Identifiers, numbers of primitive and contracted functions, and the corresponding contraction patterns are shown. Spherical Gaussians are used throughout. [b] Polarization functions are denoted by superscript *.

and implementation of the MCSCF linear response calculations[56] of the **J** tensors was originally described by Vahtras et al.;[10] it has been applied successfully for a number of times after that.[22,57,58] The GIAO SCF and MCSCF response calculation of the $\boldsymbol{\sigma}$ tensors was implemented to DALTON by Ruud et al.[17] and applied in refs 41, 58, 59, and 60. We refer to the original papers for details.

The calculation of molecular magnetic properties demands the use of relatively large atomic orbital (AO) basis sets. The sets developed by Kutzelnigg and co-workers[61] on the basis of the work by Huzinaga[62] have been found to provide converged or nearly converged shieldings and spin−spin couplings. We used two sets in our present calculations, HIII and HIV detailed in Table 2.

The HIV set was used for the calculations of ethene and ethyne, apart from one correlated calculation for the former where the smaller HIII set was employed to check the basis set convergence. The calculations of ethane were restricted to the use of the HIII set due to disk space limitations.

The choice of the MCSCF molecular orbital (MO) active spaces used was based on natural orbital occupation numbers (eigenvalues of the spin-reduced single particle density matrix) calculated using second-order many-body perturbation theory (MP2). The MP2 occupation gives a rough estimate of the importance of the various MOs for electron correlation effects. The active spaces are specified in Table 3.

For all the molecules we have kept the core MOs arising from the carbon 1*s* AOs inactive. The percentage of holes (as obtained from the MP2 natural orbital occupation analysis) recovered with these choices of active spaces is approximately 98.5 for each molecule. Two single-reference restricted active space (RAS) wave functions are used for ethane. Single and double excitations are allowed from all the occupied valence MOs to the virtual (unoccupied in the single-determinantal SCF picture) MOs. For a saturated hydrocarbon such as ethane we do not expect any significant advantage from using a multireference wave function. The amount of MP2 particles recovered by the active spaces of RAS−I and RAS−II are 87.7 and 96.3%, respectively.

For ethene we used four RAS functions. The single-reference RAS−I and the multireference RAS−II utilize an active space that recovers 91.3% of the MP2 particles. In RAS−II, the lowest unoccupied MO consisting of the carbon out-of-plane 2*p* AOs is placed to the RAS2 subspace together with the occupied valence MOs (all applicable Slater determinants are constructed within RAS2). The MP2 occupation of this MO is rather high, and there is a clear gap in the occupation numbers to the next MOs higher in energy. One may anticipate differences between the single- and multireference calculations for this molecule. The active space common to the single-reference RAS−III and the corresponding multireference RAS−IV functions contains 95.1% of MP2 particles. In all cases single and double excitations to RAS3 are considered.

Finally, for ethyne we have used two RAS functions covering 96.5% of the MP2 particles. RAS−I is a single-reference function, while in RAS−II the two virtual MOs from the off-axis carbon 2*p* AOs are treated on an equal footing with the occupied valence MOs.

The molecular geometries used in the *ab initio* calculations are given in Table 4. The r_α(300 K) geometry of ethyne corresponds to a hypothetical nonvibrating molecule with its nuclei in the positions that are thermal averages at 300 K. The r_z geometry equals r_α(0 K). The use of r_α (or the closely related r_z) geometry is motivated by the fact that harmonic vibrational corrections to the experimental direct couplings produce orientation tensors which correspond to this geometry at the temperature in question.[48]

The CPU time need of the spin−spin coupling calculations made us use the DSO and SD contributions (and also the PSO terms for ethane) from the simplest of the present calculations and transport these as such to results from the larger wave functions, which were used to calculate the demanding FC and SD/FC terms. This approach is justified by the smallness of the transported terms and/or their relative invariance with respect to improvements in the electron correlation treatment. The SD contributions to the $\mathbf{J}_{CC}$ tensors were calculated consistently for each wave function, apart from the RAS−IV calculation for ethene. In this case the RAS−II result was used. The PSO terms were found significant for a few of the coupling tensors, consequently they were calculated consistently for each wave function and each coupling in the cases of ethene and ethyne.

Results and Discussion

Experimental Spin−Spin Coupling Tensors. NMR spectra of partially oriented molecules yield spin−spin couplings as well as *D* couplings. However, as the number of adjustable

(56) Jørgensen, P.; Jensen, H. J. Aa.; Olsen, J. *J. Chem. Phys.* **1988**, *89*, 3654−61. Olsen, J.; Yeager, D. L.; Jørgensen, P. *J. Chem. Phys.* **1989**, *91*, 381−8.

(57) (a) Barszczewicz, A.; Jaszuński, M.; Kamienska-Trela, K.; Helgaker, T.; Jørgensen, P.; Vahtras, O. *Theor. Chim. Acta* **1993**, *87*, 19−28. (b) Barszczewicz, A.; Helgaker, T.; Jaszuński, M.; Jørgensen, P.; Ruud, K. *J. Chem. Phys.* **1994**, *101*, 6822−8. (c) Ruud, K.; Helgaker, T.; Jørgensen, P.; Bak, K. L. *Chem. Phys. Lett.* **1994**, *226*, 1−10. (d) Barszczewicz, A.; Helgaker, T.; Jaszuński, M.; Jørgensen, P.; Ruud, K. *J. Magn. Reson.* A **1995**, *114*, 212−8. (e) Kirpekar, S.; Jensen, H. J. Aa.; Oddershede, J. *Chem. Phys.* **1994**, *188*, 171−81.

(58) Vaara, J.; Kaski, J.; Jokisaari, J.; Diehl, P. *J. Phys. Chem. A* **1997**, *101*, 5069−81.

(59) Jaszuński, M.; Bak, K. L.; Jørgensen, P.; Helgaker, T.; Ruud, K.; Jensen, H. J. Aa. *Chem. Phys. Lett.* **1993**, *204*, 608−10. Jaszuński, M.; Helgaker, T.; Ruud, K.; Bak, K. L.; Jørgensen, P. *Chem. Phys. Lett.* **1994**, *220*, 154−60. Barszczewicz, A.; Jaszuński, M.; Helgaker, T.; Ruud, K. *Chem. Phys. Lett.* **1996**, *250*, 1−8.

(60) Vaara, J.; Oikarinen, K.; Jokisaari, J.; Lounila, J. *Chem. Phys. Lett.* **1996**, *253*, 340−8. Koskela, T.; Ylihautala, M.; Vaara, J.; Jokisaari, J. *Chem. Phys. Lett.* **1996**, *261*, 425−30. Lounila, J.; Vaara, J.; Hiltunen, Y.; Pulkkinen, A.; Jokisaari, J.; Ala-Korpela, M.; Ruud, K. *J. Chem. Phys.* **1997**, *107*, 1350−61.

(61) Kutzelnigg, W.; Fleischer, U.; Schindler, M. In *NMR Basic Principles and Progress*; Diehl, P., Fluck, E., Günther, H., Kosfeld, Eds.; Springer-Verlag: Berlin, 1990; Vol. 23, pp 165−262.

(62) Huzinaga, S. *Approximate Atomic Functions*; University of Alberta, Edmonton, 1971.

Table 3. Active Molecular Orbital Spaces in the *Ab Initio* Calculations[a]

molecule	wf	active space[b]	single/multiref[c]	n_{SD}
C_2H_6	SCF	(72/−/−/−)		1
	RAS−I	(20/−/52/14,6)	S	14265
	RAS−II	(20/−/52/25,15)	S	56371
C_2H_4	SCF	(3210 1100/−/−/−)		1
	RAS−I	(1100 0000/−/2110 1100/5522 4311)	S	3725
	RAS−II	(1100 0000/−/2111 1100/5521 4311)	M	41513
	RAS−III	(1100 0000/−/2110 1100/7644 5421)	S	7327
	RAS−IV	(1100 0000/−/2111 1100/7643 5421)	M	87853
C_2H_2	SCF	(3210 1000/−/−/−)		1
	RAS−I	(1100 0000/−/2110 1000/6633 3311)	S	3255
	RAS−II	(1100 0000/−/2111 1100/6632 3211)	M	144017

[a] The identifier of the wave function and the number of the contained Slater determinants, n_{SD}, are shown. [b] Using the nomenclature (inactive/RAS1/RAS2/RAS3),[63] where the maximum number of holes (particles) in RAS1 (RAS3) is presently limited to two. The occupation of orbitals in RAS2 is unrestricted. C_2H_6 is calculated in the Abelian C_s point group, and the numbers in each category denote the orbitals belonging to A′ and A″ symmetry species. C_2H_4 and C_2H_2 are calculated in the D_{2h} point group; the numbers denote orbitals belonging to A_g, B_{1u}, B_{2u}, B_{3g}, B_{3u}, B_{2g}, B_{1g}, and A_u symmetry species. [c] Single-reference (multireference) calculation indicated with S (M).

Table 4. Molecular Geometries Used in the *Ab Initio* Calculations[a]

molecule	geometry	r_{CC}	r_{CH}	HCC angle
C_2H_6[b]	r_z	1.5351	1.0940	111.17
C_2H_4[c]	r_z	1.3376	1.0883	121.42
C_2H_2[d]	r_α(300 K)	1.20692	1.0598	180.00

[a] Bond lengths in Å and angles in deg. r_{CC} was also fixed to the indicated value in the analysis of the experimental data. [b] Experimental geometry from ref 64. [c] Theoretical geometry from ref 53. [d] Reference 65.

parameters (chemical shifts, J and D couplings) increases, the accuracy achievable in the analysis may decrease significantly. Therefore, it is often better to determine the J couplings in the isotropic phase of the LC solvents using sample temperatures just above the isotropic−nematic phase transition. Other possibilities are to increase the concentration of the solute or to add a further component to the solution in order to destroy the mesophase. The first approach was applied here.

The observed J couplings of ethane, ethene, and ethyne measured in the isotropic phase of the solvents are given in Table 5. Each homonuclear J coupling (except the intramethyl $^2J_{HH}$ for ethane) is, in principle, measurable both in isotropic and anisotropic phases. In practice, however, the lower resolution in the spectra recorded in the anisotropic phases prevents the determination of accurate values in many cases. Those couplings that could be determined in the two phases were found to be in good mutual agreement. The table shows that the J couplings are only slightly solvent dependent. However, even a small deviation from the true value may introduce a very large error in the anisotropic properties of the **J** tensor as they are determined from a small difference between the experimental and calculated D couplings.

For the determination of the anisotropic properties of the $\mathbf{J}_{CC}$ tensors, all the dipolar couplings, D_{ij}^{exp}, were determined from the ^{1}H NMR spectra of ethane, ethene, and ethyne in several LC solvents. The couplings are collected in Table 6. The rotation around the CC bond in ethane leads to averaging of the intermethyl HH couplings so that only one coupling, $^3D_{HH}$ (respectively $^3J_{HH}$), is detectable. Thus, the observable dipolar couplings are $^1D_{CH}$, $^1D_{CC}$, $^2D_{HH}$, $^2D_{CH}$, and $^3D_{HH}$. For ethene and ethyne, the complete sets of six ($^1D_{CH}$, $^2D_{CH}$, $^1D_{CC}$, $^3D_{HH}$(*cis*), $^3D_{HH}$(*trans*) and $^2D_{HH}$(*gem*)) and four ($^1D_{CH}$, $^2D_{CH}$, $^1D_{CC}$ and $^3D_{HH}$) couplings, respectively, are observable.

For ethane and ethyne, eq 5 transforms into the simple form

$$T^{aniso} = (2/3)P_2(\cos\theta)\Delta T S_{zz}{}^D \quad (6)$$

because of the high symmetry of the molecules. $S_{zz}{}^D = S_{zz}/P_2(\cos\theta)$ is the order parameter of the CC bond (the principal symmetry axis) with respect to **n**. Due to the D_{2h} point group symmetry of ethene, two order parameters, S_{zz} and $S_{xx} - S_{yy}$, must be introduced:

$$T^{aniso} = (2/3)P_2(\cos\theta)[\Delta T S_{zz}{}^D + {}^1/_2(T_{xx} - T_{yy})(S_{xx}{}^D - S_{yy}{}^D)] \quad (7)$$

The resulting ΔJ values for ethane and ethene, along with $J_{xx} - J_{yy}$ for the latter, are given in Table 7.

The results of the current *ab initio* calculations (discussed below) indicate that ${}^1/_2{}^1J_{CH}{}^{aniso}$ and ${}^1/_2{}^2J_{CH}{}^{aniso}$ in ethyne are relatively large (about a hundred times larger than the experimental error in D) and, consequently, contribute to the corresponding experimental direct couplings. Furthermore, as we are interested in the anisotropic properties of the CC coupling tensors, also D_{CC} has to be excluded from the group of couplings used in the analyses. Not only the anisotropic contributions but also the interdependence of the dipolar couplings, as proved by experiments and theoretical treatment,[51] prevent the simultaneous estimation of the structural parameters and deformational effects on the D couplings because the problem becomes underdetermined. Therefore, alternative procedures have to be considered and applied to linear systems.

It has been shown that not only the r_α structure but also deformational contributions are additive in linear molecules.[48,51] Consequently, it is possible to write relations between the experimental dipolar couplings corrected only for harmonic vibrations. Using eq 2 and the relation $r_{CH} = r_{HH} - r'_{CH}$, where r'_{CH} is the C≡C−H distance, one can derive the following formula for the $^1D_{CH}$ coupling (assuming that ΔJ_{HH} is vanishingly small)

$$ {}^1p_{CH}[{}^1D_{CH}{}^{exp} - (1/3)\Delta^1J_{CH}S_{zz}] = \{(\gamma_H/\gamma_C)^{1/3}({}^1p_{HH}{}^1D_{HH}{}^{exp})^{-1/3} - [{}^2p_{CH}({}^2D_{CH}{}^{exp} - (1/3)\Delta^2J_{CH}S_{zz})]^{-1/3}\}^{-3} \quad (8)$$

where the ${}^np_{ij}$ values are harmonic correction factors. Once this relation is satisfied, the CC coupling anisotropy can be evaluated from

Table 5. Experimental and Theoretical Spin−Spin Couplings (Hz) of Ethane, Ethene, and Ethyne in the Isotropic Phase of the Liquid Crystal Solvents Used[a]

molecule	solvent	$^1J_{CH}$	J_{CC}	$^2J_{HH}$	$^2J_{CH}$	$^3J_{HH}$[b]
C_2H_6	I	125.190(3)	34.558(6)		−4.655(3)	8.002(2)
	II	125.200(2)	34.544(4)		−4.658(2)	8.0048(12)
	III	125.206(2)	34.521(3)		−4.657(2)	8.0030(10)
	IV	125.206(3)	34.511(5)		−4.661(2)	7.992(2)
	V	125.238(7)	34.498(15)		−4.660(7)	7.994(6)
	ab initio[d]	119.8	38.8	−14.1	−5.3	7.2[c]
C_2H_4	I	156.302(11)	67.54(2)	2.23(3)	−2.408(11)	11.62(2)
						19.02(2)
	II	156.311(7)	67.473(11)	2.37(2)	−2.428(7)	11.640(11)
						19.034(9)
	III	156.302(7)	67.457(11)	2.394(12)	−2.403(8)	11.657(11)
						19.015(9)
	IV	156.307(12)	67.45(2)	2.39(2)	−2.378(9)	11.66(2)
						18.992(15)
	V	156.312(6)	67.483(8)	2.382(13)	−2.427(6)	11.651(8)
						19.024(7)
	VI	156.309(10)	67.620(12)	2.32(3)	−2.415(9)	11.653(12)
						18.997(11)
	ab initio[e]	147.7	70.2	0.9	−3.3	10.4
						17.0
C_2H_2	I	248.29(3)	169.819(14)		49.26(3)	9.469(13)
	II	248.23(4)	169.78(4)		49.24(4)	9.51(4)
	III	248.18(3)	169.73(2)		49.23(3)	9.43(2)
	IV	248.12(3)	169.63(2)		49.20(3)	9.413(9)
	ab initio[d]	232.1	181.2		50.1	10.8

[a] The data are based on the ^{13}C NMR spectra taken at $T = 360$ K. For the composition of the liquid crystals, see the Experimental Section. [b] Two values for ethene: the upper value is for the *cis* and the lower for the *trans* coupling. [c] The average (1/3) $\Sigma_{H'} J_{HH'}$ (H′ = 1, 2, and 3) where H and H′ belong to different methyl groups, is given due to the internal rotation of the molecule. [d] RAS−II calculations. [e] RAS−IV calculation.

Table 6. Experimental *D* Couplings for Ethane, Ethene, and Ethyne in Various Liquid Crystals[a]

C_2H_6

LC	$^2D_{HH}$	$^3D_{HH}$	$^1D_{CH}$	$^2D_{CH}$	$^1D_{CC}$
I	−338.548(2)	134.565(2)	−206.474(3)	61.690(4)	67.46(2)
II	−310.609(2)	123.601(2)	−190.914(5)	56.632(5)	61.95(2)
III	571.579(2)	−227.7623(14)	354.417(4)	−104.251(4)	−113.92(2)
IV	535.632(3)	−213.863(2)	336.311(6)	−97.750(5)	−106.85(2)
V	635.666(2)	−252.905(2)	389.414(4)	−115.871(4)	−126.771(14)

C_2H_4

LC	$^2D_{HH}$	$^3D_{HH}$(*cis*)	$^3D_{HH}$(*trans*)	$^1D_{CH}$	$^2D_{CH}$	$^1D_{CC}$
I	14.992(4)	359.750(5)	118.433(5)	294.492(5)	115.655(6)	143.849(11)
II	−25.533(6)	314.743(7)	100.304(8)	221.505(11)	99.752(9)	125.72(3)
III	127.71(1)	−543.758(11)	−166.067(12)	−304.46(2)	−169.23(2)	−216.38(6)
IV	239.811(7)	−468.169(7)	−131.797(8)	−140.931(9)	−140.911(9)	−185.76(4)
V	21.769(3)	−683.698(3)	−220.455(4)	−511.040(4)	−217.703(4)	−272.805(13)
VI	71.841(4)	346.370(6)	118.103(5)	331.720(6)	112.929(7)	138.161(12)

C_2H_2

LC	$^1D_{CH}$	$^2D_{CH}$	$^3D_{HH}$	$^1D_{CC}$
I	3304.180(14)	362.359(14)	460.78(2)	597.80(3)
II	2476.89(3)	272.00(3)	345.76(4)	449.20(6)
III	−3486.53(4)	−383.26(4)	−487.35(4)	−633.88(8)
IV	−1828.36(6)	−202.13(7)	−256.71(7)	−336.61(11)

[a] The values (in Hz) were obtained from ^1H NMR spectra. The figures in parentheses indicate one standard error in units of the last digit quoted.

$$\Delta J_{CC} = 3\{p_{CC}D_{CC}^{\ exp} - [2(\gamma_H/\gamma_C)^{1/3}\,[^2p_{CH}(^2D_{CH}^{\ exp} - (1/3)\Delta^2 J_{CH}\,S_{zz})]^{-1/3} - (\gamma_H/\gamma_C)^{2/3}(p_{HH}D_{HH}^{\ exp})^{-1/3}]^{-3}\}/S_{zz} \quad (9)$$

or from

$$\Delta J_{CC} = 3\{p_{CC}D_{CC}^{\ exp} - [(\gamma_H/\gamma_C)^{2/3}(p_{HH}D_{HH}^{\ exp})^{-1/3} - 2(\gamma_H/\gamma_C)^{1/3}[^1p_{CH}(^1D_{CH}^{\ exp} - (1/3)\Delta^1 J_{CH}\,S_{zz})]^{-1/3}]^{-3}\}/S_{zz} \quad (10)$$

As there is not sufficiently independent experimental information available, it is not possible to determine the coupling anisotropies Δ^1J_{CH}, Δ^2J_{CH}, and ΔJ_{CC} from eqs 9 and 10 by keeping them as adjustable parameters. Therefore, we assumed for Δ^2J_{CH} a certain fixed value and determined the $^1p_{CH}$ from eq 8 (the additivity relation 8 is not sensitive to the other *p* values). Thereafter, the ΔJ_{CC} was calculated from eqs 9 and 10. This was repeated for several values of Δ^2J_{CH}. The mean of the ΔJ_{CC} values derived from eq 9 on one hand and from eq 10 on the other hand are in good mutual agreement, but the scatter in the values (determined for individual LC solvents) is remarkably larger in the latter case. The experimentally

Table 7. Experimental Anisotropic Properties of CC Spin−Spin Coupling Tensor in Ethane and Ethene[a]

solvent	$\Delta J_{CC}/C_2H_6$	$\Delta J_{CC}/C_2H_4$
I	57	7
II	61	21
III	61	13
IV	51	10
V	49	13
VI		3
av	56	11
ab initio	32.1	26.5

[a] Values in Hz. The experimental and calculated $J_{CC,xx} - J_{CC,yy}$ of ethene are −44 and −44.3 Hz, respectively.

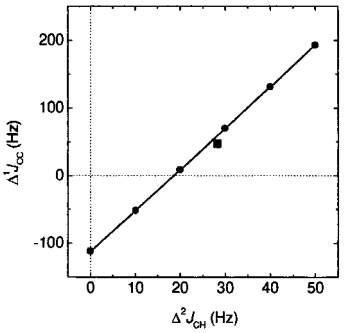

Figure 1. The experimental (−●−) interdependence of the mean of the ΔJ_{CC} values and the $\Delta 2J_{CH}$ values and the calculated *ab initio* result (■) for ethyne.

obtained interdependence of the mean (from eq 9) of the ΔJ_{CC} values and the $\Delta^2 J_{CH}$ values is displayed in Figure 1 together with the best theoretical result (seen as one ($\Delta^2 J_{CH}$, ΔJ_{CC}) point). A least-squares linear fit to the experimental points leads to $\Delta J_{CC} = 6.107 \times \Delta\ ^2J_{CH} - 112.7$ Hz (the experimental points are located on a line in the range shown in the figure). The *ab initio* calculated combination of the anisotropies is quite near to the experimental line. It should be pointed out here that if we choose $\Delta^2 J_{CH} = 28.2$ Hz ± 10%, equal to the *ab initio* value, the $\Delta\ J_{CC}$ will be in the range 42.3−76.7 Hz if calculated from the experimental linear equation. With $\Delta^2 J_{CH} = 28.2$ Hz, we get the result $\Delta J_{CC} = 59.5$ Hz. This is relatively close to the *ab initio* result $\Delta J_{CC} = 47.5$ Hz. Consequently, eqs 8−10 are satisfied with spin−spin coupling anisotropies which match well with the calculated ones. The reanalysis of the data by van der Est et al.[28] yields results that deviate only slightly from ours. Finally, it should be emphasized that the $\Delta^1 J_{CH}$ value depends critically on the harmonic vibrational correction factor $^1p_{CH}$. Because of this interdependence and the uncertainty in $^1p_{CH}$, the experimental anisotropy of the one-bond CH coupling remains an open question.

ΔJ_{CC} in ethene was obtained by the MASTER analysis correspondingly to the method previously applied to benzene[22] except that the CH bond length and the HCH angle were adjustable parameters in this case. Also the asymmetry parameter η_{CH} of the interaction tensor $\mathbf{A}_{CH}$ (these quantities are intrinsic to the deformational analysis[5]) was fixed to zero.[26] Once the various contributions are known, the anisotropic contribution is obtained from

$$J_{ij}^{\text{aniso}} = 2[D_{ij}^{\text{exp}} - (D_{ij}^{\text{eq}} + D_{ij}^{\text{h}} + D_{ij}^{\text{d}})] = 2(D_{ij}^{\text{exp}} - D_{ij}^{\text{calc}}) \quad (11)$$

The indirect contributions to the D_{CC}^{exp} values, i.e., $D_{ij}^{\text{exp}} - D_{ij}^{\text{calc}}$ in eq 11, for ethene in the seven LC solvents are results of separate MASTER calculations. In the determination of $\mathbf{J}_{CC}$ tensor we constrained the asymmetry parameter, $(J_{CC,xx} - J_{CC,yy})/J_{CC,zz}$, to be the same in different solvents. ΔJ_{CC} and $J_{CC,xx} - J_{CC,yy}$ were obtained by least-squares fitting the asymmetry parameter and the mean value of the anisotropy (the latter parameter was allowed to vary between different solvents) in the group of equations formed by introducing each experimental J_{CC}^{aniso} and the corresponding elements of the molecular orientation tensor to eq 7. This method puts all the noise of the parameters to the values of the anisotropy. However, this was not avoidable, and the mean value of ΔJ_{CC} is statistically reliable, too.

The determination of ΔJ_{CC} in ethane is a rather complicated task as MASTER in its present form is not able to handle internal rotation. This deficiency was overcome by setting the harmonic force constants related to the internal large-amplitude torsional motion to zero and calculating the rotational effects as presented in the Appendix. When all the resulting direct couplings, except for the CC coupling, are fitted to be equal with the experimental D_{ij} values, the anisotropic part of J_{CC} is given by eq 11. The corresponding anisotropies of ethane in different LC solvents are given in Table 7.

B. *Ab Initio* Spin−Spin Coupling Tensors. The calculated spin−spin coupling constants and the anisotropies of the corresponding tensors (with respect to the CC bond direction) for all the present molecules, along with the combination $J_{xx} - J_{yy}$ for ethene, are given in Tables 8 (ethane), 9 (ethene), and 10 (ethyne).

Ethane. We do not obtain information on the basis set convergence for ethane, as only the HIII set was used. On the basis of earlier experience, the use of the HIII set should not be a major limiting factor. Between our two calculations, RAS−I and RAS−II, the changes in the calculated couplings and anisotropies are generally quite small, of the order of 2−3% or below. This indicates excellent convergence. Exceptions to this rule are $^2J_{HH}$, $^2J_{CH}$, and $\Delta^2 J_{CH}$, where up to 10% changes are observed. Apart from the parameters for the $\mathbf{J}_{CC}$ tensor, the magnitude of the *J* couplings and anisotropies always decreases in the better calculation (RAS−II) as compared to the smaller one. In comparison with the experimental data (Tables 5 and 7), the RAS−II calculation performs reasonably well. The deviations from the experimentally available coupling constants (J_{CC}, $^1J_{CH}$, $^2J_{CH}$ and the average $^3J_{HH}$) are of the order of 10%, while the experimental ΔJ_{CC} from the present work is consistently slightly larger than our calculated result. It must be noted that the treatment of the internal rotation of ethane performed in the analysis of the experimental couplings introduces uncertainties mainly through its use of geometrical relaxation parameters, and the present level of agreement can be considered rather satisfactory.

The contributions of the different physical mechanisms to the **J** tensors in ethane are also listed in Table 8. The FC contribution is found to overwhelmingly dominate all the coupling constants, while SD/FC emerges as the most important contribution in the anisotropies. For couplings other than CC, the latter fact arises from the cancellation of the PSO and DSO contributions. The SD contributions are small and can generally be neglected.

Malkin *et al.*[11a] and Dickson and Ziegler[11b] performed density-functional calculations of the *J* coupling constants, while Galasso[8a] used the EOM method. The accuracy of all these first principles calculations is comparable with our RAS−II calculation, apart from the rather clear underestimation of $^2J_{CH}$ by the DFT method. Buckingham and Love[38] predicted the anisotropy of $\mathbf{J}_{CC}$ over a C−C single bond to be 34.1 Hz which

Table 8. Results of the MCSCF Calculations for the Spin−Spin Coupling Tensors in Ethane[a]

property	RAS−I/ total	RAS−II/ total	DSO	PSO	SD	FC	SD/ FC
$E + 79$	−0.527564	−0.582771					
J_{CC}	38.7	38.8	0.1	0.2	1.0	37.5	
ΔJ_{CC}	32.0	32.1	3.3	−2.3	1.5		29.6
$^1J_{CH}$	122.0	119.8	0.5	1.2	−0.2	118.4	
Δ^1J_{CH}	6.1	6.0	−6.3	4.8	0.1		7.4
$^2J_{HH}$	−14.8	−14.1	−2.9	3.0	0.4	−14.7	
Δ^2J_{HH}	−8.5	−8.3	−7.5	5.2	−0.4		−5.6
$^2J_{CH}$	−5.9	−5.3	−0.3	0.4	0.1	−5.4	
Δ^2J_{CH}	−1.9	−1.8	2.3	−1.3	0.1		−2.9
$^3J_{HH}$(a)[b]	3.6	3.5	−0.9	0.8	0.1	3.5	
Δ^3J_{HH}(a)[b]	1.6	1.6	4.0	−2.9	0.1		0.4
$^3J_{HH}$(b)[c]	14.9	14.7	−3.1	3.0	0.0	14.7	
Δ^3J_{HH}(b)[c]	3.2	3.2	1.0	−0.5	−0.1		2.8
$^3J_{HH}$(av)[d]	7.4	7.2	−1.6	1.6	0.1	7.2	
Δ^3J_{HH}(av)[d]	2.2	2.2	3.0	−2.1	0.0		1.2

[a] Calculations performed with the HIII basis set at the r_z geometry.[64] Results in Hz. The anisotropy is defined as $\Delta J = J_{zz} - {}^1/_2 (J_{xx} + J_{yy})$. The contributions of the different physical mechanisms to the calculated tensors are indicated for the RAS−II calculation. The DSO, PSO, and SD contributions to the tensors are always calculated at the RAS−I level. The total energies of the calculations are also shown (in Ha). [b] Between hydrogens belonging to different methyl groups and at *trans*-position to each other. [c] As in footnote *b* but for hydrogens at *gauche*-position to each other. [d] Rotational average of the $^3\mathbf{J}_{HH}$ tensor: $^3J_{HH}(av) = (2^3J_{HH}(a) + {}^3J_{HH}(b))/3$ and similarly for $\Delta^3J_{HH}(av)$.

is in an excellent agreement with our RAS−II estimate, 32.1 Hz. The estimate by Nakatsuji *et al.*[39a] is slightly smaller, 23.5 Hz. Pyykkö and Wiesenfeld[40] used the relativistically parametrized extended Hückel (REX) theory and obtained $\Delta J_{CC} =$ 16.3 Hz. The INDO (intermediate neglect of differential overlap) calculations of Facelli and Barfield[39c] produced also an excellent anisotropy of 30.2 Hz, with the orbital, spin-dipolar, and SD/FC cross-term contributions matching roughly with our present results.

Ethene. In the case of ethene, the convergence of both the single- and multireference series of calculations, RAS−I → RAS−III and RAS−II → RAS−IV, respectively, is good. The changes on entering the RAS−III and RAS−IV levels in both categories are only a few percent, except for the very small $^2J_{HH}$ coupling where large relative changes take place and $^2J_{CH}$ where the changes are of the order of 10%. The anisotropic properties of the **J** tensors are particularly well-converged. The difference between the single- and multireference wave functions can be seen by comparing, e.g., RAS−I and RAS−II calculations (similar changes are apparent between RAS−III and RAS−IV). The changes are relatively small in the *J* couplings but larger in the anisotropic properties. For the one-bond couplings and $^2\mathbf{J}_{HH}$, the use of a multireference function increases ΔJ and decreases $J_{xx} - J_{yy}$ by 15−25% and 3−16%, respectively. For the two- and three-bond couplings with the C═C double bond in the coupling path, both anisotropic parameters decrease by 12−30%. Comparison of the single-reference RAS−III and multireference RAS−IV (with the same active MO space as in RAS−III) results with the experimental coupling constants does not indicate very clearly which of the two wave functions is better. For J_{CC} and the difficult $^2J_{HH}$ and $^2J_{CH}$, the multireference function is superior, but the latter two couplings are still relatively far from the experimental numbers. As our main interest is in the calculation of the $\mathbf{J}_{CC}$ tensor, we tend to prefer the RAS−IV calculation which overestimates J_{CC} by 4%. The theoretically obtained anisotropic properties of this tensor are in a qualitative agreement with the present experimental data: ΔJ_{CC} is overestimated, while $J_{CC,xx} - J_{CC,yy}$ is in an excellent agreement with the LC NMR result. As these two parameters are both immersed in one experimental observable, J_{CC}^{aniso} (the two are distinguishable by using the experimental knowledge of the orientation tensor), no conclusions can be drawn to the direction that the calculations would be more successful for one of the parameters. Instead, we think that both the parameters are equally well calculated, and the good agreement of their sign and order of magnitude with the experiment verifies our calculation.

The RAS−II calculation (all contributions but the SD one) was performed both using the HIV and the smaller HIII basis set. Our main object, the $\mathbf{J}_{CC}$ tensor, is well-converged as the J_{CC} constant decreases by 2.4% and the two anisotropic parameters change by well less than 1% upon employing the larger set. The $\mathbf{J}_{CH}$ tensors display a slightly greater sensitivity to the basis, with one of the anisotropic parameters changing by 5%, and the largest effects are seen in the $\boldsymbol{J}_{HH}$ tensors. In all cases the absolute changes are quite small, however, and the HIII set can be considered a fairly converged one.

As apparent from Table 9, the FC contribution dominates the coupling constants, apart from the small $^2J_{HH}$. For J_{CC}, PSO and SD mechanisms are important, too. Similarly the SD/FC contribution is very important for the anisotropic properties of $^1\mathbf{J}_{CH}$, $^2\mathbf{J}_{HH}$, $^2\mathbf{J}_{CH}$, and $^3\mathbf{J}_{HH}$, often due to simultaneous cancellation of the DSO and PSO terms. For the anisotropic properties of the $\mathbf{J}_{CC}$ tensor, SD/FC and PSO are seen to be equally important. This and the fact that also the SD contribution is non-negligible, are qualitatively different from the situation in ethane.

The spin−spin coupling constants have been reported for ethene by the EOM,[8a] equation-of-motion coupled cluster singles and doubles (EOM-CCSD)[37] methods and DFT.[11] Among these, the EOM-CCSD results appear to compare best with the experimental data; they are superior to our own RAS−IV calculations. Unfortunately Perera et al. did not report any data for $\mathbf{J}_{CC}$ in ethene.[37] DFT and RAS−IV perform comparably, but the former appears, again, to have problems with underestimated $^2J_{CH}$. The early EOM calculations[8a] are slightly inferior. Galasso and Fronzoni[8b] reported $\Delta J_{CC} = 1.3$ Hz using the EOM theory and a 6-31G** basis set. Our 25.5 Hz is likely to be more trustworthy, partly because of the better basis set used presently. The performance of the EOM method appears to be slightly worse for ethene than ethane. The corresponding degradation is avoidable by using a proper choice of the active MO space in MCSCF calculations. For ΔJ_{CC} over the C═C double bond, Buckingham and Love[38] obtained 51.5 Hz and Nakatsuji *et al.*[39a,b] 38.7 Hz, both larger than the present RAS−IV result and experiment. REX calculations[40] result in 33.2 Hz. INDO[39c] results in $\Delta J_{CC} = 17.1$ Hz in fair agreement with our RAS−IV datum. The deviation appears to be mainly due to the underestimated SD/FC term in the semiempirical calculation.

Ethyne. For ethyne, the multireference RAS−II and single-reference RAS−I calculations produce significantly different results for the anisotropies of couplings involving hydrogen. The CC coupling parameters are found to be largely unchanged, however. We prefer the RAS−II results, which are in a relatively good agreement with the experimental data. The largest deviation of 13% is in J_{HH}. Again, the analysis of the experimental data for the anisotropic properties (detailed above) is complicated, but the calculated anisotropies ΔJ_{CC} and Δ^2J_{CH} match reasonably well with the experimental results, expressed in the form of a linear equation for the two parameters. Apart from $^1\mathbf{J}_{CH}$, the contributions (Table 10) from other than the FC

Table 9. Results of the MCSCF Calculations for the Spin−Spin Coupling Tensors in Ethene[a]

property	RAS−I/total	RAS−II/total	RAS−III/total	RAS−IV/total	DSO	PSO	SD	FC	SD/FC
$E + 78$	−0.343242	−0.352440	−0.368566	−0.379194					
J_{CC}	75.5	71.7	73.8	70.2	0.1	−8.7	3.1	75.7	
ΔJ_{CC}	21.5	25.9	22.2	26.5	5.0	7.5	−3.3		17.3
$J_{CC,xx} - J_{CC,yy}$	−56.9	−45.7	−55.8	−44.3	−0.1	−22.7	−4.1		−17.5
$^1J_{CH}$	150.9	148.9	149.8	147.7	0.4	0.5	0.0	146.8	
Δ^1J_{CH}	2.0	2.5	2.1	2.6	−2.5	2.3	−1.6		4.4
$^1J_{CH,xx} - {}^1J_{CH,yy}$	−32.6	−29.7	−31.9	−28.8	14.5	−11.0	0.8		−33.1
$^2J_{HH}$	−0.6	0.4	−0.1	0.9	−3.8	4.1	0.4	0.3	
Δ^2J_{HH}	4.3	5.2	4.4	5.3	−9.3	8.2	0.7		5.7
$^2J_{HH,xx} - {}^2J_{HH,yy}$	15.9	15.4	15.7	15.3	13.4	−9.4	0.8		10.5
$^2J_{CH}$	−5.4	−3.9	−4.9	−3.3	−0.7	−0.9	0.1	−1.9	
Δ^2J_{CH}	6.0	5.3	6.0	5.2	3.1	0.3	1.0		0.8
$^2J_{CH,xx} - {}^2J_{CH,yy}$	9.0	6.6	8.5	6.0	0.7	−5.0	−0.9		11.3
$^3J_{HH}$(*cis*)	11.7	10.8	11.3	10.4	−1.0	0.8	−0.1	10.8	
Δ^3J_{HH}(*cis*)	5.1	4.2	5.0	4.0	6.4	−4.5	0.2		1.9
$^3J_{HH,xx} - {}^3J_{HH,yy}$(*cis*)	−1.7	−1.3	−1.7	−1.2	−1.8	1.0	0.0		−0.6
$^3J_{HH}$(*trans*)	18.3	17.5	17.8	17.0	−3.5	3.1	0.4	17.0	
Δ^3J_{HH}(*trans*)	6.1	5.2	5.9	5.0	2.2	−1.4	0.4		3.7
$^3J_{HH,xx} - {}^3J_{HH,yy}$(*trans*)	−1.3	−0.9	−1.2	−0.8	2.9	−3.5	0.6		−0.9

[a] Calculations performed with the HIV basis set at the r_z geometry.[53] Results in Hz. The anisotropy is defined as $\Delta J = J_{zz} - {}^1/_2(J_{xx} + J_{yy})$ with the CC bond in the *z* direction and the molecule in the *xz* plane. The contributions of the different physical mechanisms to the calculated tensors are indicated for the RAS−IV calculation. The DSO and SD contributions to the tensors are always calculated at the RAS−I level, apart from the SD contribution to the $\mathbf{J}_{CC}$ tensor which was treated at the indicated level for RAS−II and RAS−III. For RAS−IV, the result from RAS−II was used. The total energies of the calculations are also shown (in Ha).

Table 10. Results of the MCSCF Calculations for the Spin−Spin Coupling Tensors in Ethyne[a]

property	RAS−I	RAS−II[b]	DSO	PSO	SD	FC	SD/FC
$E + 77$	−0.124289	−0.145120					
J_{CC}	191.8	181.2	0.0	6.1	8.6	166.5	
ΔJ_{CC}	46.3	47.5	6.8	54.4	−10.2		−3.4
$^1J_{CH}$	237.5	232.1	0.3	−0.7	0.3	232.2	
Δ^1J_{CH}	−68.0	−62.4	21.0	−21.3	4.0		−66.1
$^2J_{CH}$	48.6	50.1	−1.3	5.5	1.1	44.9	
Δ^2J_{CH}	33.4	28.2	4.6	10.3	−4.5		17.7
J_{HH}	12.4	10.8	−3.6	4.8	0.7	8.9	
ΔJ_{HH}	2.4	3.4	6.5	−2.0	−0.1		−1.0

[a] Calculations performed with the HIV basis set at the r_α(300 K) geometry.[65] Results in Hz. The anisotropy is defined as $\Delta J = J_{zz} - {}^1/_2(J_{xx} + J_{yy})$ with the CC bond at the *z* direction. [b] The contributions of the different physical mechanisms to the calculated tensors are indicated for the RAS−II calculation. The DSO and SD contributions to the tensors are always calculated at the RAS−I level, apart from the SD contribution to the $\mathbf{J}_{CC}$ tensor which is calculated at the indicated level. The total energies of the calculations are also shown (in Ha).

mechanism to the calculated couplings are very important in ethyne. This is very clear for the anisotropies ΔJ, where the PSO term overwhelmingly dominates ΔJ_{CC} and is large also for $\Delta^2 J_{CH}$. The DSO term dominates ΔJ_{HH}.

We find that our MCSCF calculations perform comparably with earlier wave function[8a,36] and DFT calculations[11b] for the *J* constants. The DFT results of Malkin *et al.*[11a] are better than our data, however, as observed earlier with benzene.[22] The EOM result of Galasso and Fronzoni[8b] for $\Delta J_{CC} = -4.32$ Hz is well below the range of our results, contrary to the REX value 88.8 Hz.[40] The early estimates of ΔJ_{CC} over the C≡C triple bond are 85.0 Hz[39a,b] and 99.3 Hz.[38] Facelli and Barfield[39c] calculated the rather good 33.8 Hz, where the individual mechanisms for the anisotropy correspond well to our calculations.

Table 11 shows the principal values and orientation of the PAS of the $\mathbf{J}_{CC}$ tensors in ethane, ethene, and ethyne. In each case the PAS is fixed by the symmetry, and the largest element is in the direction of the CC bond.

Table 11. Theoretical Principal Values and the Orientation of the Principal Axis Systems of the J_{CC} Tensors in Ethane, Ethene, and Ethyne[a]

molecule	J_{33}[b]	J_{22}	J_{11}
C_2H_6	60.2	28.1	28.1
C_2H_4	87.9	83.6[c]	39.2
C_2H_2	212.9	165.3	165.3

[a] In Hz. Calculations are RAS-II for ethane and ethyne, and RAS-IV for ethene. The principal values have been ordered as $|J_{33}| \geq |J_{22}| \geq |J_{11}|$. [b] In the direction of the CC bond. [c] Perpendicular to the plane of the molecule.

C. One-Bond CC Coupling Tensors and Hybridization. Figure 2 illustrates the properties of the $\mathbf{J}_{CC}$ tensor as a function of the hybridization of the carbon atoms. There are two entries for the sp^2 hybridized case: ethene calculated presently and benzene from ref 22. While the coupling constant J_{CC} displays monotonic behavior (panel (a)), the anisotropy ΔJ_{CC} with respect to the CC bond direction (b) has a minimum for the sp^2 hybridization. Whereas most of the properties of ethene and benzene appear generally very similar, there is a clear difference in ΔJ_{CC}, partly due to the fact that the large benzene molecule was calculated using rather small basis set and active MO space.[22] Panels (c) and (d) show the relative contributions from the different physical mechanisms to J_{CC} and ΔJ_{CC}. The FC mechanism dominates the coupling constant and there are no clear trends as a function of the hybridization for this property. On the contrary, for the anisotropy, the SD/FC contribution decreases drastically from sp^3 to sp^1 whereas the PSO contribution shows a strong trend in the opposite direction.[8b,39b,c]

D. Experimental Nuclear Shielding Tensors. Equations 6 and 7, **T** representing a nuclear shielding tensor, give the anisotropic contributions to the experimentally observable shielding. Equation 6, which is valid for a molecule with at least a 3-fold symmetry axis (as ethane and ethyne in the present case), shows that the anisotropy of the shielding tensor, $\Delta\sigma$, can be solved for by changing either the molecular order parameter, S_{zz}^D, or the $P_2(\cos\theta)$ factor. The situation for a molecule with only a 2-fold symmetry axis (ethene) is different. First, the change of the P_2 factor renders only the determination of a certain combination of the shielding and orientation tensor elements possible. Thus, the term in the square brackets in eq

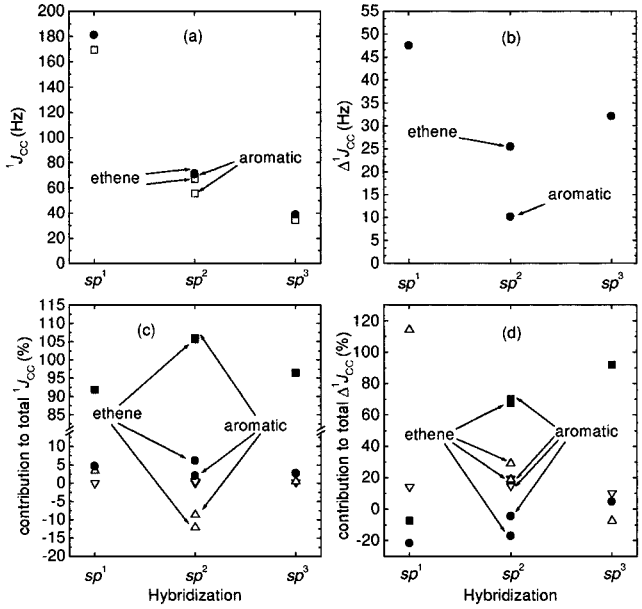

Figure 2. Properties of the $\mathbf{J}_{CC}$ tensor as a function of carbon hybridization; sp^3 from C_2H_6, sp^2 from C_2H_4 and C_6H_6,[22] and sp^1 from C_2H_2. (a) Experimental (□) and theoretical (●) spin−spin coupling constants J_{CC}. (b) Theoretical anisotropies ΔJ_{CC} with respect to the CC bond direction. (c) Relative contributions from the different physical mechanisms to the theoretical J_{CC}: DSO (▽), PSO (△), SD (●), and FC (■). (d) Relative contributions from the different physical mechanisms to the theoretical ΔJ_{CC}: symbols as in (c) except SD/FC (■).

7 can be determined but not the anisotropy, $\Delta\sigma$, nor the difference $\sigma_{xx} - \sigma_{yy}$. To obtain the latter, the ratio of the order parameters, $(S_{xx} - S_{yy})/S_{zz}$, has to be changed. A sufficiently large change cannot usually be produced by varying sample temperature: one has to use different LC solvents. This, however, may express a severe problem as solvent effects have to be properly overcome.

For ethane and ethyne, the ENEMIX[45] method provides the most suitable way to determine the $\Delta\sigma$ because the chemical shifts corresponding to parallel and perpendicular orientations of **n** with respect to $\mathbf{B}_0$ are obtained by extrapolation to the same physical state, and thus the solvent effects (both on geometry and shielding tensor) can be minimized.[66] The method is based on the fact that changing the composition of a binary mixture of two LCs with ($\Delta\chi_m < 0$ in one component and $\Delta\chi_m > 0$ in the other) makes it possible to rotate the LC director by 90°. The order parameter S_{zz}^D in eq 6 remains unchanged, but the P_2 factor jumps from 1 to $-1/2$ or *vice versa* at the point of extrapolation depending upon the direction of the approach. Using the notation $S_{zz}(\theta) = S_{zz}^D P_2(\cos\theta)$, the shielding anisotropy of the ^{1}H or ^{13}C nuclei is obtained from

$$\Delta\sigma = -(3/2)[\delta^{exp}(0°) - \delta^{exp}(90°)]/[S_{zz}(0°) - S_{zz}(90°)] \quad (12)$$

where δ^{exp} is the experimental chemical shift measured relative to the internal $^{13}CH_4$ reference, and 0° and 90° refer to the cases $\mathbf{n} \parallel \mathbf{B}_0$ and $\mathbf{n} \perp \mathbf{B}_0$, respectively.

Table 12. Experimental and *Ab Initio* Results for the Nuclear Magnetic Shielding Tensors in Ethane, Ethene, and Ethyne[a]

molecule	nucleus	method	σ	$\Delta\sigma$	$\sigma_{xx} - \sigma_{yy}$[b]
C_2H_6[cd]	C	SCF	182.1	12.1	
		RAS−I	187.0	13.0	
		RAS−II	184.7	12.5	
		LC NMR[e]	184.20	16.70	
		solid-state NMR[f]	179.3	7.0	
	H	SCF	31.05	1.13	
		RAS−I	30.85	1.17	
		RAS−II	30.92	1.21	
		LC NMR[e]	29.97	2.02	
C_2H_4[d]	C	SCF	58.0	35.7	−260.3
		RAS−I	68.2	26.0	−238.2
		RAS−II	73.6	23.2	−225.0
		RAS−III	68.1	25.4	−235.8
		RAS−IV	74.4	21.3	−220.2
		LC NMR[e]	68.27	10.76	−220.7
		LC NMR[g]	67.81	22.99	−238.0
		solid-state NMR[h]	62.1	9.0	−210
	H	SCF	26.08	5.39	−2.77
		RAS−I	26.06	4.88	−2.23
		RAS−II	26.18	4.64	−1.84
		RAS−III	26.22	4.81	−2.13
		RAS−IV	26.28	4.50	−1.63
		LC NMR[e]	25.47	3.97	−1.7
		LC NMR[g]	25.48	3.70	−1.39
C_2H_2[i]	C	SCF	115.3	244.6	
		RAS−I	121.7	235.9	
		RAS−II	126.1	229.7	
		LC NMR[e]	118.66	239.29	
		solid-state NMR[j]	118.1	240.0	
		LC NMR[k]		245	
		LC NMR[l]	118.1	253	
	H	SCF	30.39	15.81	
		RAS−I	30.32	15.81	
		RAS−II	30.28	15.87	
		LC NMR[e]	28.79	17.09	
		LC NMR[m]		14.2(3)	
		LC NMR[k]		22(2)	

[a] Results in ppm. The anisotropy is defined as $\Delta\sigma = \sigma_{zz} - {}^1/_2(\sigma_{xx} + \sigma_{yy})$ with the CC bond at the *z* direction. The HIV basis set is used in the calculated results unless otherwise noted. The total energies of the SCF calculations are (in Ha) as follows: C_2H_6: −79.261 963; C_2H_4: HIII −78.065 337; HIV −78.067 700; C_2H_2: HIII −76.850 082; HIV −76.853 508. [b] The ethene molecule is in the *xz* plane. [c] The HIII basis set used. [d] At the r_z geometry.[52,53] [e] Present experiments. [f] Reference 33. [g] Reference 32. [h] Reference 34. [i] At the r_α(300 K) geometry.[65] [j] Reference 35. [k] Reference 31. [l] Reference 30. [m] Reference 68.

A different approach has to be applied for ethene. In this case, the experimentally obtainable chemical shift can be represented in the form (see eq 7)

$$\delta^{exp} = \delta^{iso} - (2/3)P_2(\cos\theta)\,[\Delta\sigma S_{zz}{}^D + {}^1/_2(\sigma_{xx} - \sigma_{yy})(S_{xx}{}^D - S_{yy}{}^D)] \quad (13)$$

from which the two unknown variables, $\Delta\sigma$ and $\sigma_{xx} - \sigma_{yy}$, are solved using a least-squares fit to the six sets (one for each solvent) of experimental data. The elements of the order tensor are obtained from MASTER analyses based on the experimental *D* couplings. For the carbon chemical shift, the solvent effects are taken into account by adopting the δ_C^{iso} from the isotropic spectra. For the protons, solvent effect was observed to be negligible within experimental errors. The experimental results for proton and carbon shielding tensors of ethane, ethene, and ethyne are given in Table 12.

E. *Ab Initio* Nuclear Shielding Tensors. The results of the *ab initio* calculations for the shielding tensors in the molecule-fixed frame are also given in Table 12. Table 13 lists the principal components of the shielding tensors.

(63) Roos, B. O. In *Lecture Notes in Quantum Chemistry*; Roos, B. O., Ed.; Springer-Verlag: Berlin, 1992; pp 177−254.
(64) Hirota, E.; Endo, Y.; Saito, S.; Yoshida, K.; Yamaguchi, I.; Machida, K. *J. Mol. Spectrosc.* **1981**, *89*, 285−95.
(65) Lounila, J. unpublished results. The r_α(300 K) geometry is based on the r_e geometry of ref 72 and the anharmonic vibrational calculations of ref 48.
(66) Lounila, J.; Ala-Korpela, M.; Jokisaari, J. *J. Chem. Phys.* **1990**, *93*, 8514−23.

Table 13. Principal Values and the Orientation of the Principal Axis Systems of the Shielding Tensors[a]

molecule	nucleus	method	σ_{33}	σ_{22}	σ_{11}
C_2H_6	C	RAS−II	193.0[b]	180.5	180.5
		LC NMR[c]	195.33	178.63	178.63
		solid-state NMR[g]	184	177	177
	H	RAS−II	37.42[d]	28.62	26.72[e]
		MP2[f]	37.32	28.34	26.37
C_2H_4	C	RAS−IV	177.4[h]	88.5[i]	−42.8
		LC NMR[j]	179.16	83.14	−58.86
		LC NMR[c]	175.03	75.44	−45.67
		solid-state NMR[k]	164.1	68.1	−45.9
	H	RAS−IV	29.41[l]	25.60[m]	23.84
		MP2[f]	29.18	25.54	23.45
C_2H_2	C	RAS−II	279.2[n]	49.5	49.5
		LC NMR[c]	278.19	38.90	38.90
		solid state NMR[o]	278.1	38.1	38.1
		LC NMR[p]	286.8	33.8	33.8
	H	RAS−II	40.85[n]	24.99	24.99
		MP2[f]	29.98	24.71	24.71

[a] Principal values in ppm. The principal values have been ordered as $\sigma_{11} \leq \sigma_{22} \leq \sigma_{33}$. [b] The most shielded direction along the CC bond. [c] Present experiments. [d] The most shielded direction makes an angle of 53.54° with the CC bond direction, while the $\mathbf{r}_{CH}$ vector is at 68.83° with the same direction. The conversion of the tensor in PAS to some molecular fixed frame is possible with the eq $\sigma_{\alpha\beta} = \sum_{ab} \cos\theta_{a\alpha} \cos\theta_{b\beta}\sigma_{ab}$, where $\theta_{a\alpha}$ is the angle between positive a and α axis. Note that the conversion from LC NMR data to PAS is not necessarily possible due to lack of information. [e] The least shielded direction normal to the plane of local site symmetry at the H nucleus. [f] Reference 42. [g] Reference 33. Converted to the absolute scale using value $\sigma_C^{iso} =$ 188.1 ppm for TMS.[67] [h] The most shielded direction perpendicular to the plane of the molecule. [i] In the direction of the CC bond. [j] Reference 32. [k] Reference 34. [l] The most shielded direction makes an angle of 8.67° with the CC bond direction, while the $\mathbf{r}_{CH}$ vector is at 58.58°. [m] Perpendicular to the plane of the molecule. [n] The most shielded direction along the CC bond. [o] Reference 35. [p] Reference 30.

Information on the basis set convergence was obtained from the calculations of C_2H_4 and C_2H_2 at the SCF level and C_2H_4 at the RAS−II level. In these cases the calculations were repeated using the HIII basis set (results not shown). The ^{13}C and ^{1}H shielding constants change by less than 1% from the HIII to HIV basis for each calculation. The only significant change observed for the ^{13}C shielding tensor is the 1.4% decrease in $\Delta\sigma_C$ for C_2H_4 at the RAS−II level. The HIV basis set can be considered to be relatively converged for carbon. The ^{1}H tensor is more difficult to calculate to the same relative accuracy.[42] Despite the good convergence of the shielding constants, the anisotropic parameters $\Delta\sigma_H$ and $\sigma_{H,xx} - \sigma_{H,yy}$ for C_2H_4 change by +2 to +3% from HIII to HIV, and the HIV set may not be fully converged, as observed earlier.[58] For ethyne the change in $\Delta\sigma_H$ is below 0.5%, though.

Ethane. For ethane, the series of SCF and the two single-reference RAS calculations RAS−I and RAS−II show reasonable convergence. The RAS−I calculation with the relatively small active space overshoots the correlation contribution to the ^{13}C shielding observables, as the RAS−II with larger active space gives a correction in the opposite direction. The final σ_C is in a very good agreement with experiment, but this may be partly coincidental as the harmonic vibrational effects are not considered in the calculations. The $\Delta\sigma_C$ is underestimated as compared to the experimental result, but generally of acceptable accuracy when considering the magnitude of the absolute error. The CCSD σ_C of Gauss and Stanton, 186.5 ppm,[44] is calculated at the experimental r_e geometry, which probably explains most of the difference with our RAS−II calculation at the r_z geometry. At the r_z geometry the main effects of the anharmonic vibrations are incorporated.[48] For comparison, Grayson and Raynes[43] reported SCF data of the $\boldsymbol{\sigma}_C$ tensor, from which $\Delta\sigma_C = 11.4$ ppm can be obtained.

The present σ_H appears to converge to a higher value than the experimental result. The best MP2 result of Chesnut,[42] 30.68 ppm, is slightly better than ours, presumably due to the very extended basis set and different geometry used in that reference. The best present calculation for the anisotropy results in 1.21 ppm, whereas the experimental result is 2.0 ppm. The relative difference is large, but the absolute error is quite small: the experimental result contains solvent contributions which may produce uncertainties of this magnitude.

Ethene. The correlation contribution to the $\boldsymbol{\sigma}$ tensors in ethene is large, as evident from the comparison of SCF and RAS−I or RAS−II calculations. There is also a significant difference between single- (RAS−I and RAS−III) and multi-reference (RAS−II and RAS−IV) calculations: the latter ^{13}C shielding constant is 5−6 ppm higher than the former. Among the two categories of reference functions, the series SCF → RAS−I → RAS−III is reasonably converged when reaching the RAS−III level with 33 virtual orbitals in the RAS3 subspace. The convergence of the corresponding multireference series appears to be slightly inferior, e.g., the $\Delta\sigma_C$ decreases by 8.4% and $\sigma_{H,xx} - \sigma_{H,yy}$ by 11.5% from RAS−II to RAS−IV. In comparison with the experimental data, the single-reference function RAS−III gives σ_C in a very good agreement with the experiment, whereas the anisotropic properties of the $\boldsymbol{\sigma}_C$ tensor are worse than those from the multireference RAS−IV calculation. The experimental $\Delta\sigma_C$ and $\sigma_{C,xx} - \sigma_{C,yy}$ are sensitive to the details of the analysis, however. In analogy with what was noted above for $\mathbf{J}_{CC}$ in ethene, the discrepancy of what we believe to be our best current calculation, RAS−IV, with the experiment in the former and excellent agreement in the latter case may be accidental. The theoretically obtained parameters are, nevertheless, of the correct sign and order of magnitude for carbon and very good for hydrogen. For comparison, the ^{13}C shielding constant calculated using the CCSD method at r_e is 71.3 ppm,[44] midway between our RAS−III and RAS−IV calculations. It is expected that the rovibrational contribution to σ_C is of the order of −2 ppm;[65] consequently the CCSD result appears to be a very good one. It is evident that a still larger active MO space than in RAS−IV is necessary to obtain a quantitatively accurate ^{13}C shielding tensor for C_2H_4 using MCSCF calculations. The tensorial properties of $\boldsymbol{\sigma}_C$ at the SCF level are similar to those reported earlier.[43] As with ethane, the earlier MP2 calculation with a large basis set is slightly better than our RAS−IV, giving $\sigma_H = 26.06$ ppm.[42]

Ethyne. The single- and multireference calculations for C_2H_2 with the same active space, RAS−I and RAS−II, expectedly produce different results. The correlation contributions to σ_C are +6.4 and +10.8 ppm for RAS−I and RAS−II, respectively. The latter is believed to be the better of the two RAS functions. The final results for σ_C and $\Delta\sigma_C$ are in a satisfactory but not excellent agreement (within a few percent) with the experimental data. As with C_2H_4, the CCSD result at r_e, $\sigma_C = 121.8$ ppm,[44] appears to need only the vibrational corrections for quantitative accuracy. Our RAS−II result is 4 ppm above this value. The complete active space (CAS) calculation by Rizzo et al.[41] utilized understandably a smaller active space than ours and resulted in $\sigma_C = 129.1$ ppm and $\Delta\sigma_C = 225.0$ ppm.

For hydrogen shieldings in C_2H_2 the correlation contributions are small. The MP2 result for σ_H is the rather good 29.98 ppm, while the $\Delta\sigma_H$ is the same as our SCF result, 15.81 ppm.[42] The CAS results,[41] $\sigma_H = 30.5$ ppm and $\Delta\sigma_H = 15.6$ ppm, are comparable to our RAS−II, too.

Conclusions

We have determined the indirect $\mathbf{J}_{CC}$ coupling tensors for carbons with different hybridizations in the simple hydrocarbons, C_2H_6, C_2H_4, and C_2H_2. The anisotropies of the tensors are all positive according to both experimental and theoretical investigations. We could also for the first time extract the asymmetry term of indirect coupling tensor, $J_{CC,xx} - J_{CC,yy}$ for ethene. Moreover, this study gives the first reliable experimental information on the non-negligible anisotropic contribution to the indirect CH coupling ever. The signs and magnitudes of the experimentally and theoretically determined indirect coupling parameters are in a good mutual agreement which confirms the reliability of the results. The present MCSCF calculations of the coupling tensors use large active molecular orbital spaces, the restricted active space scheme and both single- (all molecules) and multireference (ethene and ethyne) wave functions. The results for the coupling constants are comparable to earlier first principles work, but our data for the anisotropic properties of the tensors are the best reported so far for these molecules. Still better results could probably be obtained by tailoring the one-particle basis sets and better treatment of dynamical correlation, e.g., by using larger active spaces. We studied also the nuclear shielding properties. Again, we found a good mutual agreement between these independently determined tensors. The same reference functions were used for shieldings as for the coupling tensors. The present set of both isotropic and anisotropic data is reliable but slightly inferior in comparison with recent CCSD calculations for the carbon shielding constants[44] and MP2 results for the principal values of the ^{1}H tensors.[42] Finally, this work shows that the anisotropic part of indirect coupling, $^1/_2J_{CC}^{aniso}$, for these molecules is less than 1% of the corresponding direct coupling. Together with the previous result for benzene (the contribution was less than 2%)[22] we can state that the contribution of CC indirect coupling is small compared to the direct coupling. Consequently, it can be ignored to a reasonable accuracy in the determination of structure and orientation of a molecule dissolved in liquid crystal phases.

Acknowledgment. The authors are grateful to the Academy of Finland for financial support. Jyrki Schroderus is thanked for the calculation of the vibration−rotation wave functions of ethane. We are grateful to Dr. Juhani Lounila for important conversations about molecular deformations. J.K. would like to express his gratitude to the Alfred Kordelin Fund. Kenneth Ruud, University of Oslo, is thanked for access to the DALTON software and running the RAS-IV shielding calculation for ethene. Center for Scientific Computing (CSC, Espoo, Finland) provided the computational resources.

Appendix

The effects arising from the internal rotation of ethane on the analysis of the D couplings were calculated quantum mechanically. The MASTER program was applied to evaluate the contributions D^h and D^d for each coupling at fixed angles $\phi = n \times 10°$ (n = 0, 1, ..., 6) of the internal rotation (corresponding to rigid conformation). In further calculations it should be noticed that the period in the contributions to the intermethyl HH couplings (in the given pair of protons) is 360°, whereas it is 120° in the others (the situation reverts to the starting point after 120° due to symmetry). These periods are used for describing the effects with Fourier series. On the basis of symmetry arguments, the harmonic and deformational contributions are, however, obtained by only considering a 60 degree rotation. The contributions due to deformation depend on the internal rotation and on the anisotropies ΔA_{CH} and ΔA_{CC} of the interaction tensors. The asymmetry parameter, η_{CC}, is zero due to CC rotation and η_{CH} is assumed to be small; therefore it is neglected in the analysis. The deformational contribution can be represented in the form[5b]

$$D_{ij}^{\,d} = [a_{ij}(\phi) + c_{ij}(\phi)\, S_{zz}]\Delta A_{CH} + [b_{ij}(\phi) + d_{ij}(\phi)S_{zz}]\Delta A_{CC} \quad (14)$$

where, as the first step, the coefficients a_{ij}, b_{ij}, c_{ij}, and d_{ij} with the fixed value of ϕ are solved for using a least-squares fit to five outputs of the MASTER program produced by using five different fixed combinations of ΔA_{CH} and ΔA_{CC}. The second step is the introduction of the rotational effects on the coefficients. This is made by determining the coefficients of the first five terms of a Fourier series on the basis of seven sets of the a, b, c, and d values corresponding to the seven values of ϕ. The harmonic contributions change also with the rotation and are taken into account by the equation

$$D_{ij}^{\,h} = e_{ij}(\phi)S_{zz} \quad (15)$$

where the coefficient e is only weakly dependent on the rotation, except for intermethyl HH coupling. The coefficients in eqs 14 and 15 are given as Supporting Information in Table S1.

The coupling D_{ij}^{eq} in eq 3 changes during the internal rotation for each pair of nuclei i and j due to the relaxation of the molecular conformation at different ϕ.[69] This must also be taken into account as it turns out to be an important effect on the final results. The observable intermethyl direct coupling, $^3D_{HH}^{eq}(\phi)$, as a function of ϕ can be written as

$$^3D_{HH}^{\,eq}(\phi) = (1/3)\sum_i D_{1,i}^{\,eq} = -\sum_k \{K_{HH}S_{zz}[3(\Delta z/r_{1,k+4})^2 - 1]/[6r_{1,k+4}{}^3]\} \quad (16)$$

where i = 4, 5, and 6, k = 0 and 2, $K_{HH} = -\mu_0\hbar\gamma_H{}^2/8\pi^2$, and Δz is the difference of the z coordinates of the protons, $\Delta z = \Delta z(\phi) = r_{CC}(\phi) + 2r_{CH}(\phi)\cos\alpha(\phi)$, $\alpha(\phi)$ being the angle between the z axis and the CH bond. The intermethyl distance $r_{1,k+4} = r_{1,k+4}(\phi)$ between the protons 1 and (k + 4) (protons 1, 2, 3, and carbon 7 are numbered to be in the same methyl group and 4, 5, 6, and carbon 8 in the other) is given by

$$r_{1,k+4}(\phi) = \{(\Delta z(\phi))^2 + r_s{}^2(\phi)[\cos(2k\pi/3 + \phi) - 1]^2 + r_s{}^2(\phi)\sin^2(2k\pi/3 + \phi)\}^{1/2} \quad (17)$$

where k = 0, 1, 2 and r_s is the distance of the proton from the z axis, $r_s(\phi) = r_{CH}(\phi)\sin\alpha(\phi)$.

Once the direct couplings and the harmonic and deformational contributions to them are known as a function of rotational angle, the average coupling is given by

$$\langle D_{ij}\rangle = \int_0^{\pi/3} D(\phi)\, p(\phi)\, d\phi \quad (18)$$

where $D(\phi)$ is the direct coupling as a function of the internal rotation angle and $p(\phi)$ is the corresponding normalized probability distribution function. In the quantum mechanical calculation of the latter, the eigenstates with energies ($E = E_v + E_t$ where v stands for vibration and t for torsion) correspond-

(67) Jameson, A. K.; Jameson, C. J. *Chem. Phys. Lett.* **1987**, *134*, 461.
(68) Montana, A. J.; Dailey, B. P. *Mol. Phys.* **1975**, *30*, 1521−8.
(69) Al-Kahtani, A.; Montero, S.; Nibler, J. *J. Chem. Phys.* **1993**, *98*, 101−9.

ing to wavenumbers[52] over 2000 cm^{-1} were neglected on the basis of small occupation according to Boltzmann statistics. The occupation of state i (below 2000 cm^{-1}) is given by eq

$$p_i = e^{-E_i/kT}/\sum_j e^{-E_j/kT} \tag{19}$$

where E_i is the total energy of the state. The probability distribution function of the state i is given by the corresponding wave function squared ($|\Psi_i|^2$) which was calculated using the leading torsional parameters $V_3 = 1011.89$ cm^{-1} and $V_6 = 10.77$ cm^{-1}, taken from ref 69. The calculation procedure was adopted from ref 70. The normalized probability distribution function in eq 18 is given by eq

$$p(\phi) = \sum_i p_i |\Psi_i(\phi)|^2 \tag{20}$$

where p_i is calculated using eq 19. The potential function determined for gaseous ethane obviously approximates well the potential in liquid, as no systematic change in the methyl torsional frequency on entering the liquid state has been detected.[71] The intermethyl D_{HH} coupling is obtained from eq 18 by including the $D_{HH}^{eq}(\phi)$ from eq 16, along with the harmonic vibrational and deformational contributions, and conformational relaxation. The orientation of the molecule is calculated from the anisotropies of the interaction tensors using the equation[5b]

$$S_{CC}^{D} = 2c/15 + 4c^2/315 - 8c^3/4725 - 16c^4/31185 + ... \tag{21}$$

where c is the dimensionless quantity

$$c = 9A_{zz}^{e}/4k_BT \tag{22}$$

In the case of ethane, A_{zz}^{e} is calculated with equation

$$A_{zz}^{e} = 2\{\Delta A_{CC} + 6P_2(\cos[\alpha(\phi)])\Delta A_{CH}\}/3 \tag{23}$$

where the factor 6 is the number of CH bonds of ethane.

Supporting Information Available: The Fourier coefficients determining the contributions to direct couplings in ethane due to deformation and harmonic vibrations as a function of the internal rotation angle (2 pages). See any current masthead page for ordering information and Web access instructions.

JA972936M

(70) Moazzen-Ahmadi, N.; Gush, H. P.; Halpern, M.; Jagannath, H.; Leung, A.; Ozier, I. *J. Chem. Phys.* **1988**, 88, 563−77.
(71) Durig, J. *Vibrational Spectra and Structure*; Marcel Dekker: New York, 1972; Vol. 1, p 138.
(72) Bramley, M. J.; Carter, S.; Handy, N. C.; Mills, I. M. *J. Mol. Spectrosc.* **1993**, *157*, 301−36.